科学通报 2018 年 第 63 卷 第 2 期: 232 ~ 240
论 文
《中国科学》杂志社
SCIENCE CHINA PRESS

基于工质物性的热力循环性能探索

苏文, 赵力*, 邓帅

天津大学机械工程学院, 中低温热能高效利用教育部重点实验室, 天津 300072
* 联系人, E-mail: jons@tju.edu.cn

2017-06-01 收稿, 2017-07-24 修回, 2017-07-24 接受, 2017-09-28 网络版发表
国家自然科学基金(51476110)资助

摘要 工质作为热力循环实现能量转换不可或缺的载体, 其物性直接决定了循环性能的高低. 为探究工质物性对热力循环的性能影响, 首先采用立方型状态方程计算了实际工质的剩余性质, 并根据理想气体的热力性质推导了任意状态下工质的热力学参数, 进而得到了等容过程、等压过程、等温过程及绝热过程中能量的表达式. 在此基础上, 针对4个动力正循环, 即卡诺循环、朗肯循环、布雷顿循环及斯特林循环, 分别推导了循环输出功及效率的表达式, 分析了循环性能与温度、工质物性之间的关系. 针对工程应用中热力循环完善度偏低的问题, 基于状态方程及循环温熵图探索了面向工质特性的热力循环性能极限, 为热力循环的实际运行及优化设计提供了理论参考.

关键词 热力循环, 工质物性, 性能极限, 状态方程, 剩余性质

在工程应用中, 热力循环根据目的不同, 可分为动力正循环和制冷/供热逆循环. 在动力正循环中, 高温热能通过膨胀机转换为机械能. 本文针对工程中常见的动力正循环, 即朗肯循环、布雷顿循环、斯特林循环, 分析其循环过程及热力性能[1]. 同时, 任何工程热力循环的实现都离不开能流载体——工质. 工质通过热力状态的循环变化, 以实现能量的传递与转换. 因此, 热力循环的性能分析必须建立在工质物性的基础上. 此外, 在实际工程中, 即便是最好的热力循环, 与卡诺循环相比, 其循环效率也大幅偏离卡诺效率, 热力学完善度普遍小于50%. 实际循环效率不仅与传热温差, 工质流动摩擦所引起的不可逆损失有关, 还与循环的具体形式相关. 对于每一种循环形式, 可能存在一个比卡诺效率低的效率上限. 因此, 为了分析工质物性及循环形式对热力性能的影响, 本文将基于工质立方型状态方程对卡诺循环、朗肯循环、布雷顿循环及斯特林循环展开研究.

卡诺循环作为第一个被提出的理想循环, 其效率决定着实际热力循环性能的上限[2]. Agrawal和Menon[3]基于范德瓦尔斯方程得到了工质的循环效率; 郑世燕等人[4]研究了以Dieterici气体为工质的卡诺循环效率; Tjiang和Sutanto[5]采用任意气体状态方程推导了卡诺循环的效率. 上述研究结果均表明, 卡诺循环的效率只与高低温热源有关, 与工质的物性没有关系.

朗肯循环在工程中已得到广泛的应用. 目前, 火力发电厂都采用的是以水为工质的朗肯循环. 当回收工业余热、太阳能及地热能等中低温品位的热能时, 通常采用低沸点的有机物作为朗肯循环的工质[6,7]. 朗肯循环利用工质等压相变的巨大潜热从热源吸收能量, 进而在膨胀机中对外做功. 在工质选择中, 不仅要考虑朗肯循环效率, 还需考虑工质的环境特性、安全性及经济性. 近年来, 已有大量文献对有机朗肯循环的工质选择做了深入研究[8,9], 分析了工

引用格式: 苏文, 赵力, 邓帅. 基于工质物性的热力循环性能探索. 科学通报, 2018, 63: 232–240
Su W, Zhao L, Deng S. The performance of thermodynamic cycles based on the properties of working fluids (in Chinese). Chin Sci Bull, 2018, 63: 232–240, doi: 10.1360/N972017-00608

质物性如临界温度[10]、压力[11]、输运特性[12]对循环性能的影响. 然而, 在上述研究中, 工质的物性都是采用商业软件如REFPROP[13], COOLPROP[14]来调取, 其计算依据是由大量实验数据拟合建立的高精度方程, 还未见通过立方型状态方程直接表达工质的热力循环性能.

布雷顿循环为燃气轮机的热力循环, 与朗肯循环具有一样的4个热力过程, 区别在于布雷顿循环中工质不涉及相变换热. 布雷顿循环的热力性能与工质的物性直接相关, 目前研究最多的工质便是超临界CO_2[15~17]. 对于布雷顿循环, 工质物性的计算都是通过商业软件完成, 还未见到基于立方型状态方程的循环性能分析.

斯特林循环是一种回热式循环, 在工程应用中, 通常采用回热过程对余热进行回收和利用, 不但使得循环的效率得以提高, 而且还有利于节能和环保, 因此得到了广泛的应用[18,19]. 郑世燕等人[4]研究了以Dieterici气体为工质的斯特林循环性能, 并采用广义Redlich-Kwong气体为工质研究了不可逆回热式斯特林循环的输出功和效率[20]. 此外, 研究者也分别以范德瓦尔斯气体及昂尼斯气体为工质推导了斯特林循环的效率表达式[21,22].

综上所述, 对于卡诺循环、斯特林循环, 虽有基于状态方程的循环性能研究, 但都采用的是气体状态方程, 而对于朗肯循环、布雷顿循环, 至今未见基于状态方程的循环性能分析. 同时, 对于不同循环形式, 基于工质物性的循环性能极限还未曾有人研究. 因此, 本文将基于一般的立方型状态方程, 对4种热力循环的效率及输出功进行推导, 并依据循环温熵图的几何形式, 对每种循环的性能极限进行分析, 为循环性能优化及设计提供思路.

1 实际工质的热力过程分析

状态方程是压力P、体积v和温度T之间的代数关联式. 目前, 主要采用的状态方程是基于经验的立方型状态方程. 当P和T一定时, 立方型状态方程可以解析出v. 所有的立方型状态方程都可以表达为分子间斥力与引力对压力贡献的加和, 其一般通用形式为[23]

$$P=\frac{RT}{v-b}-\frac{af(T)}{(v+\delta_1 b)(v+\delta_2 b)}, \tag{1}$$

其中a是引力项中的能量参数, b是协体积参数, $f(T)$为与温度有关的能量函数, 参数δ_1, δ_2根据不同状态方程而定.

对于动力正循环, 效率的定义如下:

$$\eta=\frac{w}{q_{\text{in}}}, \tag{2}$$

其中w为循环净输出功, q_{in}为循环的吸热量. 根据能量守恒定律, 循环净输出功

$$w=q_{\text{in}}-q_{\text{out}}, \tag{3}$$

其中q_{out}为循环的放热量. 因此, 循环效率

$$\eta=1-\frac{q_{\text{out}}}{q_{\text{in}}}. \tag{4}$$

为确定热力循环中涉及的热量交换, 本文从剩余Helmholtz能出发计算工质在任意状态点之间的热力学性质差异. 根据立方型状态方程, 可得任意状态下实际工质的剩余Helmholtz能

$$a^r=\int_v^\infty (p-RT\rho)\mathrm{d}v=RT\ln\frac{v}{v-b}+\frac{af(T)}{(\delta_1-\delta_2)b}\ln\frac{v+\delta_2 b}{v+\delta_1 b}. \tag{5}$$

由此可导出任意状态下实际工质的剩余熵

$$s^r=-\left(\frac{\partial(a^r)}{\partial T}\right)_v=-R\ln\frac{v}{v-b}-\frac{af'(T)}{(\delta_1-\delta_2)b}\ln\frac{v+\delta_2 b}{v+\delta_1 b}; \tag{6}$$

工质的剩余内能

$$u^r=a^r+Ts^r=\left(\frac{af(T)}{(\delta_1-\delta_2)b}-\frac{aTf'(T)}{(\delta_1-\delta_2)b}\right)\ln\frac{v+\delta_2 b}{v+\delta_1 b}; \tag{7}$$

工质的剩余焓

$$\begin{aligned}h^r&=u^r+(p/\rho-RT)\\&=\left(\frac{af(T)}{(\delta_1-\delta_2)b}-\frac{aTf'(T)}{(\delta_1-\delta_2)b}\right)\ln\frac{v+\delta_2 b}{v+\delta_1 b}+(p/\rho-RT).\end{aligned} \tag{8}$$

根据以上导出的剩余性质, 可得工质在状态点1和2之间的熵差

$$\Delta s_{1-2}=s_2-s_1=s_2^r+(s_2^0-s_1^0)-s_1^r, \tag{9}$$

其中s_1^0, s_2^0为理想气体在状态点1和2的熵. 根据理想气体状态方程, 可得

$$s_2^0-s_1^0=\int_{T_1}^{T_2}\frac{c_v^0}{T}\mathrm{d}T+R\ln\left(\frac{v_2}{v_1}\right). \tag{10}$$

将式(6)与(10)代入式(9), 得

$$\begin{aligned}\Delta s_{1-2}=&R\ln\frac{(v_2-b)}{(v_1-b)}+\int_{T_1}^{T_2}\frac{c_v^0}{T}\mathrm{d}T-\frac{af'(T_2)}{(\delta_1-\delta_2)b}\ln\frac{v_2+\delta_2 b}{v_2+\delta_1 b}\\&+\frac{af'(T_1)}{(\delta_1-\delta_2)b}\ln\frac{v_1+\delta_2 b}{v_1+\delta_1 b}.\end{aligned} \tag{11}$$

对于状态点1和2之间的内能差, 同理可得

$$\Delta u_{1-2}=u_2-u_1=u_2^r+(u_2^0-u_1^0)-u_1^r, \tag{12}$$

其中 u_1^0,u_2^0 为理想气体在状态点1和2的内能，其差为

$$u_2^0-u_1^0=\int_{T_1}^{T_2}c_v^0\mathrm{d}T. \tag{13}$$

将式(7)与(13)代入式(12)，得

$$\begin{aligned}\Delta u_{1-2}=&\left(\frac{af(T_2)}{(\delta_1-\delta_2)b}-\frac{aT_2f'(T_2)}{(\delta_1-\delta_2)b}\right)\ln\frac{v_2+\delta_2b}{v_2+\delta_1b}\\&-\left(\frac{af(T_1)}{(\delta_1-\delta_2)b}-\frac{aT_1f'(T_1)}{(\delta_1-\delta_2)b}\right)\ln\frac{v_1+\delta_2b}{v_1+\delta_1b}+\int_{T_1}^{T_2}c_v^0\mathrm{d}T.\end{aligned} \tag{14}$$

同理可得状态点1和2之间的焓差

$$\Delta h_{1-2}=h_2-h_1=h_2^r+(h_2^0-h_1^0)-h_1^r, \tag{15}$$

其中 h_1^0,h_2^0 为理想气体在状态点1和2的焓，其差为

$$h_2^0-h_1^0=\int_{T_1}^{T_2}c_p^0\mathrm{d}T. \tag{16}$$

将式(8)与(16)代入式(15)，得

$$\begin{aligned}\Delta h_{1-2}=&\left(\frac{af(T_2)}{(\delta_1-\delta_2)b}-\frac{aT_2f'(T_2)}{(\delta_1-\delta_2)b}\right)\ln\frac{v_2+\delta_2b}{v_2+\delta_1b}\\&-\left(\frac{af(T_1)}{(\delta_1-\delta_2)b}-\frac{aT_1f'(T_1)}{(\delta_1-\delta_2)b}\right)\ln\frac{v_1+\delta_2b}{v_1+\delta_1b}\\&+(p_2v_2-RT_2)-(p_1v_1-RT_1)+\int_{T_1}^{T_2}c_p^0\mathrm{d}T.\end{aligned} \tag{17}$$

根据以上计算得到的热力性质差，可对以下4个典型的热力过程进行能量计算.

对于定容过程，根据热力学关系

$$\mathrm{d}u=T\mathrm{d}s+p\mathrm{d}v, \tag{18}$$

当v一定时，系统从外界吸收的热量

$$q_{1-2}=T\Delta s_{1-2}=\Delta u_{1-2}. \tag{19}$$

对于定压过程，依据热力学关系

$$\mathrm{d}h=T\mathrm{d}s+v\mathrm{d}p, \tag{20}$$

当压力一定时，系统从外界吸收的热量

$$q_{1-2}=T\Delta s_{1-2}=\Delta h_{1-2}. \tag{21}$$

对于定温过程，系统的吸热量

$$q_{1-2}=T\Delta s_{1-2}. \tag{22}$$

对于等熵过程，系统绝热，故

$$q_{1-2}=0. \tag{23}$$

通过以上4个过程的能量表达式，就可以推导出不同热力循环的效率及净输出功.

2 卡诺循环

卡诺循环由两个等温过程和两个等熵过程构成，其温熵变化如图1所示. 工质从热源等温吸热(1-2)，经过等熵膨胀(2-3)后，向冷源等温放热(3-4)，经过等熵压缩(4-1)回到初始状态.

由于循环吸放热量均发生在等温过程，故

$$\begin{aligned}q_{\mathrm{in}}&=T_1(s_2-s_1)\\&=T_1\left(R\ln\frac{v_2-b}{v_1-b}+\frac{af'(T_1)}{(\delta_1-\delta_2)b}\ln\frac{(v_2+\delta_1b)(v_1+\delta_2b)}{(v_2+\delta_2b)(v_1+\delta_1b)}\right),\end{aligned} \tag{24}$$

$$\begin{aligned}q_{\mathrm{out}}&=T_4(s_3-s_4)\\&=T_4\left(R\ln\frac{v_3-b}{v_4-b}+\frac{af'(T_4)}{(\delta_1-\delta_2)b}\ln\frac{(v_3+\delta_1b)(v_4+\delta_2b)}{(v_3+\delta_2b)(v_4+\delta_1b)}\right).\end{aligned} \tag{25}$$

根据等熵过程2-3, 4-1可得

$$\begin{aligned}\int_{T_2}^{T_3}\frac{c_v^0}{T}\mathrm{d}T=&\frac{af'(T_3)}{(\delta_1-\delta_2)b}\ln\frac{v_3+\delta_2b}{v_3+\delta_1b}-\frac{af'(T_2)}{(\delta_1-\delta_2)b}\ln\frac{v_2+\delta_2b}{v_2+\delta_1b}\\&-R\ln\frac{(v_3-b)}{(v_2-b)},\end{aligned} \tag{26}$$

$$\begin{aligned}\int_{T_1}^{T_4}\frac{c_v^0}{T}\mathrm{d}T=&\frac{af'(T_4)}{(\delta_1-\delta_2)b}\ln\frac{v_4+\delta_2b}{v_4+\delta_1b}-\frac{af'(T_1)}{(\delta_1-\delta_2)b}\ln\frac{v_1+\delta_2b}{v_1+\delta_1b}\\&-R\ln\frac{(v_4-b)}{(v_1-b)}.\end{aligned} \tag{27}$$

由于T_1=T_2，T_3=T_4，且理想气体的 c_v^0 只与温度有关，故依据式(26)和(27)可得

$$\begin{aligned}&R\ln\frac{v_2-b}{v_1-b}+\frac{af'(T_1)}{(\delta_1-\delta_2)b}\ln\frac{(v_2+\delta_1b)(v_1+\delta_2b)}{(v_2+\delta_2b)(v_1+\delta_1b)}\\&=R\ln\frac{v_3-b}{v_4-b}+\frac{af'(T_4)}{(\delta_1-\delta_2)b}\ln\frac{(v_3+\delta_1b)(v_4+\delta_2b)}{(v_3+\delta_2b)(v_4+\delta_1b)},\end{aligned} \tag{28}$$

则卡诺循环的效率

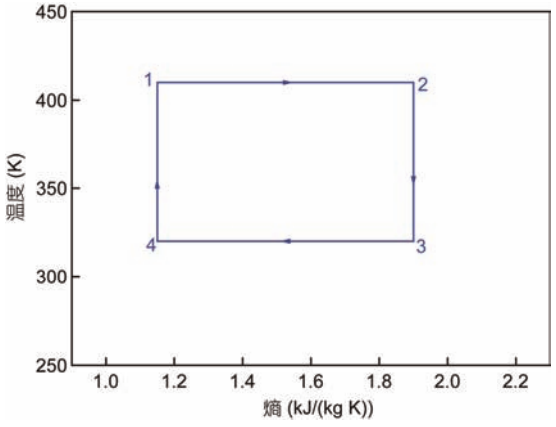

图 1 (网络版彩色)卡诺循环温熵图

Figure 1 (Color online) *T*-*s* diagram for Carnot cycle

$$\eta_{\text{carnot}}=1-\frac{T_4\left(R\ln\frac{v_3-b}{v_4-b}+\frac{af'(T_4)}{(\delta_1-\delta_2)b}\ln\frac{(v_3+\delta_1 b)(v_4+\delta_2 b)}{(v_3+\delta_2 b)(v_4+\delta_1 b)}\right)}{T_1\left(R\ln\frac{v_2-b}{v_1-b}+\frac{af'(T_1)}{(\delta_1-\delta_2)b}\ln\frac{(v_2+\delta_1 b)(v_1+\delta_2 b)}{(v_2+\delta_2 b)(v_1+\delta_1 b)}\right)}$$
$$=1-\frac{T_4}{T_1},\tag{29}$$

卡诺循环的净输出功

$$w_{\text{carnot}}=q_{\text{in}}-q_{\text{out}}$$
$$=(T_1-T_4)\left(R\ln\frac{v_2-b}{v_1-b}+\frac{af'(T_1)}{(\delta_1-\delta_2)b}\ln\frac{(v_2+\delta_1 b)(v_1+\delta_2 b)}{(v_2+\delta_2 b)(v_1+\delta_1 b)}\right).\tag{30}$$

从式(29)可以看出，卡诺效率只与热源温度有关，与工质无关，即对于任何工质，只要其做卡诺循环，其效率就是卡诺效率. 从热力学第二定律可知，该效率是任何循环的效率上限. 由式(30)可知，卡诺循环的输出功是温度和工质物性的函数，冷热源温差越大，工质在等温过程的熵差越大，则输出功就越大.

3 朗肯循环

朗肯循环由两个等压过程和两个等熵过程构成. 以工质R245fa为例，其温熵变化如图2所示. 在蒸发器中，工质从热源等压吸热，将经历预热(3-4)、蒸发(4-5)、过热(5-2)3个阶段，经过等熵膨胀做功(2-6)，工质经冷凝器等压放热，由过热乏气冷凝到过冷液(6-7-8-1). 此后，过冷液经等熵压缩回到初始状态以完成循环(1-3). 由于低温工质液体在等熵压缩中温升很小，所以图中状态点1与3很接近.

朗肯循环的吸放热发生在定压过程3-2和6-1中，故

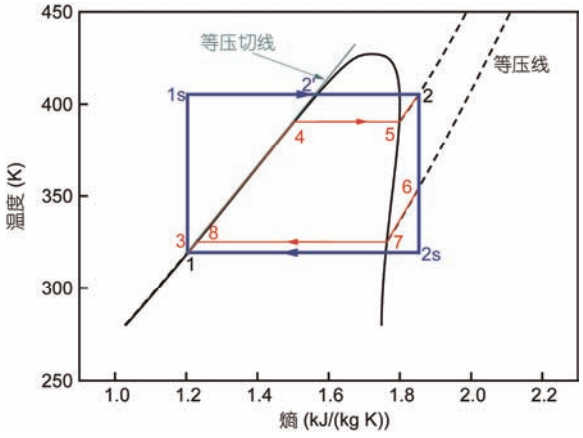

图 2 (网络版彩色)R245fa亚临界朗肯循环温熵图

Figure 2 (Color online) *T*-*s* diagram of subcritical rankine cycle for R245fa

$$q_{\text{in}}=h_2-h_3$$
$$=\left(\frac{af(T_2)}{(\delta_1-\delta_2)b}-\frac{aT_2f'(T_2)}{(\delta_1-\delta_2)b}\right)\ln\frac{v_2+\delta_2 b}{v_2+\delta_1 b}$$
$$-\left(\frac{af(T_3)}{(\delta_1-\delta_2)b}-\frac{aT_3f'(T_3)}{(\delta_1-\delta_2)b}\right)\ln\frac{v_3+\delta_2 b}{v_3+\delta_1 b}$$
$$+(p_2v_2-RT_2)-(p_3v_3-RT_3)+\int_{T_3}^{T_2}c_p^0\mathrm{d}T,\tag{31}$$

$$q_{\text{out}}=h_6-h_1$$
$$=\left(\frac{af(T_6)}{(\delta_1-\delta_2)b}-\frac{aT_6f'(T_6)}{(\delta_1-\delta_2)b}\right)\ln\frac{v_6+\delta_2 b}{v_6+\delta_1 b}$$
$$-\left(\frac{af(T_1)}{(\delta_1-\delta_2)b}-\frac{aT_1f'(T_1)}{(\delta_1-\delta_2)b}\right)\ln\frac{v_1+\delta_2 b}{v_1+\delta_1 b}$$
$$+(p_6v_6-RT_6)-(p_1v_1-RT_1)+\int_{T_1}^{T_6}c_p^0\mathrm{d}T,\tag{32}$$

则循环的效率

$$\eta_{\text{rankine}}=1-\frac{\left(\frac{af(T_6)}{(\delta_1-\delta_2)b}-\frac{aT_6f'(T_6)}{(\delta_1-\delta_2)b}\right)\ln\frac{v_6+\delta_2 b}{v_6+\delta_1 b}-\left(\frac{af(T_1)}{(\delta_1-\delta_2)b}-\frac{aT_1f'(T_1)}{(\delta_1-\delta_2)b}\right)\ln\frac{v_1+\delta_2 b}{v_1+\delta_1 b}+(p_6v_6-RT_6)-(p_1v_1-RT_1)+\int_{T_1}^{T_6}c_p^0\mathrm{d}T}{\left(\frac{af(T_2)}{(\delta_1-\delta_2)b}-\frac{aT_2f'(T_2)}{(\delta_1-\delta_2)b}\right)\ln\frac{v_2+\delta_2 b}{v_2+\delta_1 b}-\left(\frac{af(T_3)}{(\delta_1-\delta_2)b}-\frac{aT_3f'(T_3)}{(\delta_1-\delta_2)b}\right)\ln\frac{v_3+\delta_2 b}{v_3+\delta_1 b}+(p_2v_2-RT_2)-(p_3v_3-RT_3)+\int_{T_3}^{T_2}c_p^0\mathrm{d}T},\tag{33}$$

输出功

$$w_{\text{rankine}}=\left(\frac{af(T_2)}{(\delta_1-\delta_2)b}-\frac{aT_2f'(T_2)}{(\delta_1-\delta_2)b}\right)\ln\frac{v_2+\delta_2 b}{v_2+\delta_1 b}-\left(\frac{af(T_3)}{(\delta_1-\delta_2)b}-\frac{aT_3f'(T_3)}{(\delta_1-\delta_2)b}\right)\ln\frac{v_3+\delta_2 b}{v_3+\delta_1 b}+(p_2v_2-RT_2)-(p_3v_3-RT_3)+\int_{T_3}^{T_2}c_p^0\mathrm{d}T$$
$$-\left(\frac{af(T_6)}{(\delta_1-\delta_2)b}-\frac{aT_6f'(T_6)}{(\delta_1-\delta_2)b}\right)\ln\frac{v_6+\delta_2 b}{v_6+\delta_1 b}+\left(\frac{af(T_1)}{(\delta_1-\delta_2)b}-\frac{aT_1f'(T_1)}{(\delta_1-\delta_2)b}\right)\ln\frac{v_1+\delta_2 b}{v_1+\delta_1 b}-(p_6v_6-RT_6)+(p_1v_1-RT_1)-\int_{T_1}^{T_6}c_p^0\mathrm{d}T.\tag{34}$$

由于吸放热量等于相应的焓变，等熵过程2-6和1-3导出的等式无法用于化简式(33)和(34). 从效率及输出功的表达式可以看出，理想朗肯循环效率及输出功的确定需要4个状态点的温度及压力，循环性能是温度和工质的函数. 从工程应用可知，相对于卡诺循环效率，朗肯循环的热力学完善度普遍小于50%. 因此，卡诺效率对于朗肯循环的指导意义较小. 由于朗肯循环涉及工质相变，且液体工质的性质对于压力变化不敏感，相较于卡诺循环，在朗肯循环的温熵图中，工质液体侧始终存在一块不能利用的面积，即图2所示的面积$S_{1-1s-2'-1}$，其中1-2′为温熵斜率最大的等压切线. 对于朗肯循环其他未利用的面积，如$S_{4-5-2-2'-4}$，$S_{1-8-7-6-2s-1}$，可以通过选择适宜的工质和工况来逼近相应的卡诺循环过程，使其面积减少. 因此，对于朗肯循环，存在一个比卡诺循环性能低的极限热力性能. 根据图2所示，朗肯循环的极限功为

$$w_{\text{limit-rankine}} = S_{1-2'-2-2s-1} = S_{1-1s-2-2s-1} - S_{1-1s-2'-1}, \quad (35)$$

朗肯循环的极限效率为

$$\eta_{\text{limit-rankine}} = 1 - \frac{T_1}{T_2 - \frac{1}{2}(T_2 - T_1)\frac{\Delta s_{1s-2'}}{\Delta s_{1s-2}}}. \quad (36)$$

式(36)中熵差比值是循环温度及压力的函数，即

$$\frac{\Delta s_{1s-2'}}{\Delta s_{1s-2}} = f(T_1, T_2, P_1, P_2), \quad (37)$$

其中P_1，P_2分别为朗肯循环两个等压过程的压力. 从以上式子可以看出，朗肯循环的极限效率与工质的性质有关. 工质液相等压线温熵斜率越大，则其极限效率也就越高. 目前，在亚临界朗肯循环中，最接近该极限效率的循环为天津大学Li[24]提出的梯形循环，即利用工质等温相变的特性来逼近卡诺循环，从而提高循环的效率. 对于跨临界朗肯循环，亦可采用温熵斜率最大的等压切线导出极限效率，如图3所示的CO_2跨临界朗肯循环温熵图.

4 布雷顿循环

布雷顿循环的基本热力过程与朗肯循环一样，由两个等压过程和两个等熵过程构成，如图4所示的CO_2布雷顿循环温熵图. 工质从高温热源等压吸热(3-2)，经过等熵膨胀(2-4)，向低温冷源放热(4-1)，而后通过等熵压缩(1-3)回到循环初始状态，完成整个循环过程. 与朗肯循环相比，布雷顿循环的工质处在气体状态，一般为CO_2或空气.

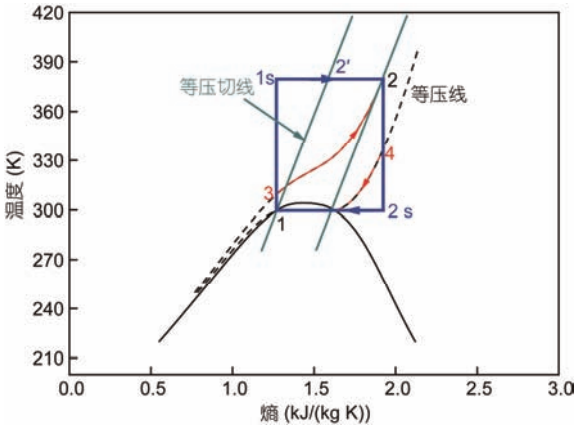

图 3 (网络版彩色)CO_2跨临界朗肯循环温熵图

Figure 3 (Color online) *T*-*s* diagram of transcritical Rankine cycle for CO_2

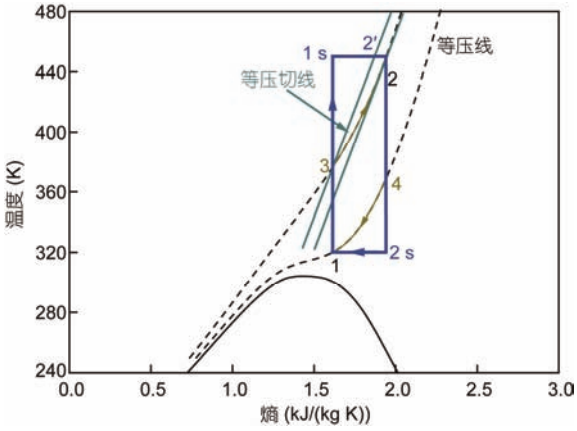

图 4 (网络版彩色)CO_2布雷顿循环温熵图

Figure 4 (Color online) *T*-*s* diagram of Brayton cycle for CO_2

由于布雷顿循环不涉及工质的相变，等压吸放热量可以通过等压热容计算，即

$$q_{\text{in}} = h_2 - h_3 = \int_{T_3}^{T_2} c_p \mathrm{d}T, \quad (38)$$

$$q_{\text{out}} = h_4 - h_1 = \int_{T_1}^{T_4} c_p \mathrm{d}T, \quad (39)$$

则循环效率为

$$\eta_{\text{brayton}} = 1 - \int_{T_1}^{T_4} c_p \mathrm{d}T \Big/ \int_{T_3}^{T_2} c_p \mathrm{d}T, \quad (40)$$

循环输出功为

$$w_{\text{brayton}} = \int_{T_3}^{T_2} c_p \mathrm{d}T - \int_{T_1}^{T_4} c_p \mathrm{d}T. \quad (41)$$

由式(40)及(41)可知，布雷顿循环性能的确定需要工质4个状态点温度参数及工质比热随温度压力的变化关系，说明该循环性能与工质有关. 同朗肯循环一样，相对于卡诺循环，布雷顿循环温熵图中也总是

存在一块不能利用的面积，即 $S_{3\text{-ls}-2'-3}$，如图4所示，其中3-2′为温熵斜率最大的等压切线. 由朗肯循环分析可知，布雷顿循环也存在着一个与工质相关，且比卡诺效率低的极限效率，其表达式如下:

$$\eta_{\text{limit-brayton}}=1-\frac{T_1}{T_2-\dfrac{1}{2}(T_2-T_3)\dfrac{\Delta s_{\text{ls}-2'}}{\Delta s_{\text{ls}-2}}}, \tag{42}$$

式(42)中熵差比值是循环温度及压力的函数.

5 斯特林循环

斯特林循环由两个等温过程和两个等容过程构成，如图5所示. 工质从高温热源等温膨胀吸热(3-2)，通过等容放热(2-4)后，又等温压缩放热(4-1)，经过等容吸热(1-3)后回到初始状态，完成整个循环过程.

对于等温过程3-2和4-1，吸放热量分别为

$$\begin{aligned}q_{3-2}&=T_2(s_2-s_3)\\&=T_2\left(R\ln\frac{v_2-b}{v_3-b}+\frac{af'(T_2)}{(\delta_1-\delta_2)b}\ln\frac{(v_2+\delta_1 b)(v_3+\delta_2 b)}{(v_2+\delta_2 b)(v_3+\delta_1 b)}\right),\end{aligned} \tag{43}$$

$$\begin{aligned}q_{1-4}&=T_1(s_4-s_1)\\&=T_1\left(R\ln\frac{v_4-b}{v_1-b}+\frac{af'(T_1)}{(\delta_1-\delta_2)b}\ln\frac{(v_4+\delta_1 b)(v_1+\delta_2 b)}{(v_4+\delta_2 b)(v_1+\delta_1 b)}\right).\end{aligned} \tag{44}$$

对于等容过程的热量交换，有

$$\begin{aligned}q_{1-3}=&\left(\frac{af(T_3)}{(\delta_1-\delta_2)b}-\frac{aT_3f'(T_3)}{(\delta_1-\delta_2)b}\right)\ln\frac{v_3+\delta_2 b}{v_3+\delta_1 b}\\&-\left(\frac{af(T_1)}{(\delta_1-\delta_2)b}-\frac{aT_1f'(T_1)}{(\delta_1-\delta_2)b}\right)\ln\frac{v_1+\delta_2 b}{v_1+\delta_1 b}+\int_{T_1}^{T_3}c_v^0\mathrm{d}T,\end{aligned} \tag{45}$$

$$\begin{aligned}q_{4-2}=&\left(\frac{af(T_2)}{(\delta_1-\delta_2)b}-\frac{aT_2f'(T_2)}{(\delta_1-\delta_2)b}\right)\ln\frac{v_2+\delta_2 b}{v_2+\delta_1 b}\\&-\left(\frac{af(T_4)}{(\delta_1-\delta_2)b}-\frac{aT_4f'(T_4)}{(\delta_1-\delta_2)b}\right)\ln\frac{v_4+\delta_2 b}{v_4+\delta_1 b}+\int_{T_4}^{T_2}c_v^0\mathrm{d}T.\end{aligned} \tag{46}$$

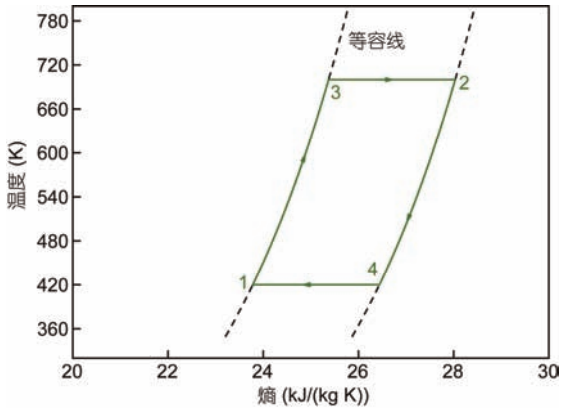

图 5 (网络版彩色)以氦为工质的斯特林循环温熵图
Figure 5 (Color online) *T*-*s* diagram of Sterling cycle for He

在斯特林循环中，常采用内置回热器的方法，使两个等体过程的吸放热量发生在工质系统内. 当吸放热量相等时，称为理想回热过程. 但对于实际工质，由于吸放热量不相等，将产生回热损失，即

$$\Delta q=q_{1-3}-q_{4-2}. \tag{47}$$

根据等温条件 $T_1=T_4$，$T_2=T_3$，等容条件 $v_1=v_3$，$v_2=v_4$，且理想气体热容 c_v^0 只与温度有关，可得回热损失为

$$\begin{aligned}\Delta q=&\left(\frac{a\left(f(T_2)-f(T_1)\right)}{(\delta_1-\delta_2)b}-\frac{a\left(T_2f'(T_2)-T_1f'(T_1)\right)}{(\delta_1-\delta_2)b}\right)\\&\cdot\ln\frac{(v_1+\delta_2 b)(v_2+\delta_1 b)}{(v_1+\delta_1 b)(v_2+\delta_2 b)}.\end{aligned} \tag{48}$$

因此，斯特林循环的输出功为

$$\begin{aligned}w_{\text{sterling}}&=q_{3-2}+\Delta q-q_{1-4}\\&=(T_2-T_1)R\ln\frac{v_2-b}{v_1-b}+\frac{a\left(f(T_2)-f(T_1)\right)}{(\delta_1-\delta_2)b}\\&\quad\cdot\ln\frac{(v_1+\delta_2 b)(v_2+\delta_1 b)}{(v_1+\delta_1 b)(v_2+\delta_2 b)},\end{aligned} \tag{49}$$

循环效率为

$$\eta_{\text{sterling}}=1-\frac{q_{1-4}}{q_{3-2}+\Delta q}=1-\frac{RT_1\ln\dfrac{v_2-b}{v_1-b}+\dfrac{aT_1f'(T_1)}{(\delta_1-\delta_2)b}\ln\dfrac{(v_2+\delta_1 b)(v_1+\delta_2 b)}{(v_2+\delta_2 b)(v_1+\delta_1 b)}}{RT_2\ln\dfrac{v_2-b}{v_1-b}+\left(\dfrac{a\left(f(T_2)-f(T_1)\right)}{(\delta_1-\delta_2)b}-\dfrac{aT_1f'(T_1)}{(\delta_1-\delta_2)b}\right)\ln\dfrac{(v_1+\delta_2 b)(v_2+\delta_1 b)}{(v_1+\delta_1 b)(v_2+\delta_2 b)}}. \tag{50}$$

从上述式子可以看出, 当工质为实际气体时, 需要两个状态点的温度及体积来计算循环输出功及效率. 当工质为理想气体时, 斯特林循环的效率为

$$\eta_{\text{ideal-sterling}} = 1 - \frac{T_1}{T_2}. \tag{51}$$

当实际气体工质越接近理想气体时, 其效率就越靠近卡诺效率. 因此, 对于斯特林循环, 其极限效率即为卡诺效率.

6 结论

本文基于工质通用立方型状态方程, 利用热力学剩余性质, 推导了任意状态下的热力学函数, 得到了等熵过程及3种等值过程中能量的表达式. 在此基础上, 分别计算了卡诺循环、朗肯循环、布雷顿循环及斯特林循环的输出功和效率, 分析了冷热源温度与工质物性对循环性能的影响. 结果表明卡诺循环的效率只与温度有关, 而卡诺循环的输出功和其他循环的热力性能均由循环的温度和工质决定. 这意味着在相同的温度区间内, 不同的工质将会有不一样的循环性能. 针对热力循环完善度较低的问题, 本文分析了各动力循环的性能极限. 对于卡诺循环及斯特林循环, 其极限效率为卡诺效率, 只与温度有关. 对于朗肯循环及布雷顿循环, 以温熵图中等压线斜率最大的切线导出了极限效率. 该极限效率比卡诺效率低, 是温度和工质的函数, 能够更好地指导热力循环的工程应用.

参考文献

1 Zeng D L, Ao Y, Zhang X M, et al. Engineering Thermodynamics (in Chinese). Beijing: Higer Education Press, 2002. 259–314 [曾丹苓, 敖越, 张新铭, 等. 工程热力学. 北京: 高等教育出版社, 2002. 259–314]

2 Laranjeiras C C, Portela S I C. The Carnot cycle and the teaching of thermodynamics: A historical approach. Phys Edu, 2016, 51: 5013–5021

3 Agrawal D C, Menon V J. The Carnot cycle with the van der Waals equation of state. Eur J Phys, 1990, 11: 88–90

4 Zheng S Y, Peng S S, Yang H S. Performance analysis of two classes of heat engines with Dieterici gas as working fluid (in Chinese). J Thermal Sci Tech, 2012, 11: 69–74 [郑世燕, 彭石狮, 杨惠山. 以 Dieterici 气体为工质的两类热机循环性能分析. 热科学与技术, 2012, 11: 69–74]

5 Tjiang P C, Sutanto S H. The efficiency of the Carnot cycle with arbitrary gas equations of state. Eur J Phys, 2006, 27: 719–726

6 Miao Z, Yang X F, Xu J L, et al. Development and dynamic characteristics of an organic Rankine cycle. Chin Sci Bull, 2014, 59: 4367–4378

7 Wu S Y, Li C, Xiao L, et al. A comparative study on thermo-economic performance between subcritical and transcritical organic Rankine cycles under different heat source temperatures. Chin Sci Bull, 2014, 59: 4379–4387

8 Su W, Zhao L, Deng S. Group contribution methods in thermodynamic cycles: Physical properties estimation of pure working fluids. Renew Sust Energy Rev, 2017, 79: 984–1001

9 Liu B T, Chien K H, Wang C C. Effect of working fluids on organic Rankine cycle for waste heat recovery. Energy, 2004, 29: 1207–1217

10 Yang L, Gong M Q, Guo H, et al. Effects of critical and boiling temperatures on system performance and fluid selection indicator for low temperature organic Rankine cycles. Energy, 2016, 109: 830–844

11 Su W, Zhao L, Deng S. Simultaneous working fluids design and cycle optimization for organic Rankine cycle using group contribution model. Appl Energy, 2017, 202: 618–627

12 Stijepovic M Z, Linke P, Papadopoulos A I, et al. On the role of working fluid properties in organic Rankine cycle performance. Appl Therm Eng, 2012, 36: 406–413

13 Lemmon E W, Huber M L, Mclinden M O. NIST standard reference database 23: Reference fluid thermodynamic and transport properties-REFPROP. 9.0. In: Proceedings of National Standard Reference Data Series. NIST, 2010

14 Bell I H, Wronski J, Quoilin S, et al. Pure and pseudo-pure fluid thermophysical property evaluation and the open-source thermophysical property library coolprop. Ind Eng Chem Res, 2014, 53: 2498

15 Wang K, He Y L, Zhu H H. Integration between supercritical CO_2 Brayton cycles and molten salt solar power towers: A review and a comprehensive comparison of different cycle layouts. Appl Energy, 2017, 195: 819–836

16 Luu M T, Milani D, McNaughton R, et al. Dynamic modeling and start-up operation of a solar-assisted recompression supercritical CO_2 Brayton power cycle. Appl Energy, 2017, 199: 247–263

17 Deng Q H, Wang D, Zhao H, et al. Study on performances of supercritical CO_2 recompression Brayton cycles with multi-objective optimization. Appl Therm Eng, 2017, 114: 1335–1342

18 Zhou Y Q. A discussion about the ideal Sterling cycle's principle of operation and factors that influence the efficiency of a real Sterling cycle (in Chinese). Phys Eng, 2015, 25: 49–52 [周雨青. 理想斯特林热机循环原理及其效率的计算和实际工作效率的简单讨论. 物理与工程, 2015, 25: 49–52]
19 Mancini T, Heller P, Butler B, et al. Dish-stirling systems: An overview of development and status. J Sol Energy T-ASME, 2003, 125: 135–151
20 Zheng S Y. Power output and efficiency of irreversible regenerative Stirling heat engine using generalized Redlich-Kwong gas as the working substance (in Chinese). Acta Phys Sin, 2014, 63: 113–120 [郑世燕. 以广义 Redlich-Kwong 气体为工质的不可逆回热式斯特林热机循环输出功率和效率. 物理学报, 2014, 63: 113–120]
21 Zhang W. The effciency of stirling heat engine with Onnes gas as working substance (in Chinese). J Kashgar Tea Col, 2013, 34: 22–25 [张伟. 以昂尼斯气体为工质的斯特林热机循环效率. 喀什师范学院学报, 2013, 34: 22–25]
22 Sun J X. Three kinds of cycle efficiency of heat engine with the van der Waals gas as working substance (in Chinese). Phys Eng, 2013, 23: 22–25 [孙久勋. 以范德瓦尔斯气体为工质的 3 种热机循环效率. 物理与工程, 2013, 23: 22–25]
23 Su W, Zhao L, Deng S. Recent advances in modeling the vapor-liquid equilibrium of mixed working fluids. Fluid Phase Equilibr, 2017, 432: 28–44
24 Li X G. A trapezoidal cycle with theoretical model based on organic Rankine cycle. Int J Energy Res, 2016, 40: 1624–1637

Summary for “基于工质物性的热力循环性能探索”

The performance of thermodynamic cycles based on the properties of working fluids

Wen Su, Li Zhao* & Shuai Deng

Key Laboratory of Efficient Utilization of Low and Medium Grade Energy, Ministry of Education, School of Mechanical Engneering, Tianjin University, Tianjin 300072, China
* Corresponding author, E-mail: jons@tju.edu.cn

With the increase of global energy demand, themodynamic cycles, such as Rankine cycle, refrigeration or heat pump, have been widely employed to generate work or transfer heat. Since these cycles generally consist of a linked sequence of state points with physical properties variables, the physical properties of working fluid are essential to the cycle analysis. They directly determine the design of components, the cycle performance, the cycle stability and safety. However, in the thermodynamic analysis, the determination of cycle performance and the calculation of required physical properties are usually seperated. The thermodynamic peroperties of working fluids are often obtained from the complex experimental equations, so that the relationship between the cycle performance and the working fluids has not been established yet. What’s more, due to the fact that Carnot efficiency doesn’t contain detailed information on the properties of working fluids, a nature idea emerges how to derive the efficiency limit under the constraint of working fluids. Thus, in this work, the influences of thermodynamic properties on power cycles are investigated and the limiting efficiencys are proposed.

In order to derive the cycle performances from the physical properties of working fluids, a general cubic equation of state is employed to obtain the residual properties, such as residual enthalpy, residual entropy and residual internal energy. Thereafter, on the basis of the properties of ideal gas, thermodynamic parameters of working fluids at any state are determined. According to the thermodynamic general relationships, the required heat is obtained for four classical processes, namely isochoric, isobaric, isothermal and isentropic processes. Based on the derived expressions, the output work and cycle efficiency are obtained for power cycles including Carnot cycle, Rankine cycle, Brayton cycle and Sterling cycle. The relationship between the cycle performance and the temperature, the properties of working fluids is developed. As a theoretical upper bound of cycle efficiency, Carnot efficiency is only determined by temperatures of heat source and sink. While the output work of Carnot cycle is a function of temperatures and the properties of working fluids. For other power cycles, it can be concluded that the thermodynamic performances are related with temperatures and working fluids, based on the derived expressions from cubic equation of state. Furthermore, compared with the Carnot efficiency under the same heat source and sink, the thermodynamic perfections of cycles are very low in practical engineering. Therefore, performance limits of thermodynamic cycles are investigated on the basis of the characteristics of working fluids in this paper. Limiting performance is derived from the equation of state and the temperature-entropy diagram of working fluids. For Rankine cycle and Brayton cycle, a maximum isobaric slope in the temperature-entropy diagram is employed to cut out the unexploited area from the enclosed area of Carnot cycle, so that the limiting work and efficiency can be obtained from the cycle areas. For Sterling cycle, when the used working fluid is ideal gas, the cycle efficiency is equal to Carnot efficiency. Although the proposed limiting performance can not be achieved by practical cycles, it can provide some theoretical guidance for the operating condition and the optimal design of thermodynamic cycles.

thermodynamic cycles, properties of working fluids, performance limit, equation of state, residual properties

doi: 10.1360/N972017-00608